Electric Power Systems Research 143 (2017) 53–65

Contents lists available at ScienceDirect

Electric Power Systems Research

journal homepage: www.elsevier.com/locate/epsr

Harmonic resonance characteristics of large-scale distributed power plant in wideband frequency domain

Zhiyong Chen*, An Luo, Huimin Kuang, Leming Zhou, Yandong Chen, Yuan Huang

College of Electrical and Information Engineering, Hunan University, Changsha, Hunan Province, China

ARTICLE INFO

Article history:
Received 17 December 2015
Received in revised form 14 July 2016
Accepted 6 September 2016

Keywords:
Distributed generation
Harmonic current
Resonance band

ABSTRACT

For the sake of systematically investigating the propagation and magnification of harmonic currents inside large-scale distributed power plants (LDPP), firstly, the model of LDPP is built, in which the topology of multiple overhead feeders, the distributed capacitances of feeders, the stray capacitances of transformers, and the control strategy of DG units are taken into account. Secondly, the model reveals the distributions and movements of several resonance bands along with the length variations of feeders. Then, these resonance bands could be classified into three basic types: extrinsic resonance band, filter resonance band, and ring resonance band. Furthermore, the ring resonance band will be in collusion with the filter resonance band at specific length of feeders. As a result, a superimposition resonance band will emerge and high harmonic currents are produced. Finally, some simulation cases and experiments are conducted to verify the correctness of the harmonic resonance modeling, also the feasibility of proposed hybrid active power filter (HAPF) to attenuate the wideband-frequency harmonic currents is testified.

1. Introduction

Distributed generation (DG) is regarded as one of the most promising forms of renewable energy utilization. Low-voltage DG units combining with energy storage system and local loads under hierarchical control [1,2] can constitute a microgrid. The microgrid can operate in both grid-connected [3,4] and islanded mode [5,6] in order to satisfy different supply demands. Several clusters of DG units of high capacity connecting with high-voltage feeders can be integrated into a large-scale distributed power plant (LDPP), such as photovoltaic plants [7] and wind farms [8], so as to achieve centralizing power transmission and high-efficiency power dispatching.

When large quantities of low-voltage DG units are integrated into a local distribution network, the power quality of the grid will be challenged [9] owing to the high penetration of DG units. The interaction of the equivalent impedance among clustering DG units and the grid will cause coupling resonances [10,11]. As a result, an extra moveable resonance peak will emerge in the output current of each DG unit [12]. This resonance peak will move toward a relatively low-frequency domain along with the growth in number of clustering DG units [3,13]. For low-voltage DG units, the consequences of low-frequency resonances are far worse than high-frequency resonances since the characteristic harmonics of inverters are around odd-order low frequencies. The cause of parallel resonances among clustering DG units is the singularity of the network admittance matrix in an extreme case [14]. When it comes to series resonances, the cause of them is the inappropriate ratio between the inverter output impedance and the grid impedance [15].

For the LDPP integrating with several clusters of DG units of high capacity, the resonance scenario is quite different. The topology of the LDPP, especially in mountainous or offshore wind farm, typically consists of several long-distance overhead feeders. A cluster of DG units connect with a high-voltage feeder through their distributed transformers (DTs), as shown in Fig. 1. Two elements greatly impact the wideband-frequency behaviors of the LDPP, including: (1) The stray capacitances in and between primary and secondary circuits of DTs; (2) The distributed capacitances of overhead feeders.

These capacitances coupling with the inductive elements inside the LDPP will provide potential low-impedance channels for harmonic currents of certain frequencies. In other words, it may cause harmonic resonances. As a consequence, the harmonic currents will be magnified during the propagation from the DG units to the collector bus of the LDPP. Besides, the grid impedance will also interact with the capacitances of the LDPP, magnifying unpleasant harmonics.

Some literatures have investigated the resonance problems associated with the LDPP. A simplified model of photovoltaic plant

* Corresponding author.
E-mail address: chenzhiyong2008bj@126.com (Z. Chen).

http://dx.doi.org/10.1016/j.epsr.2016.09.001

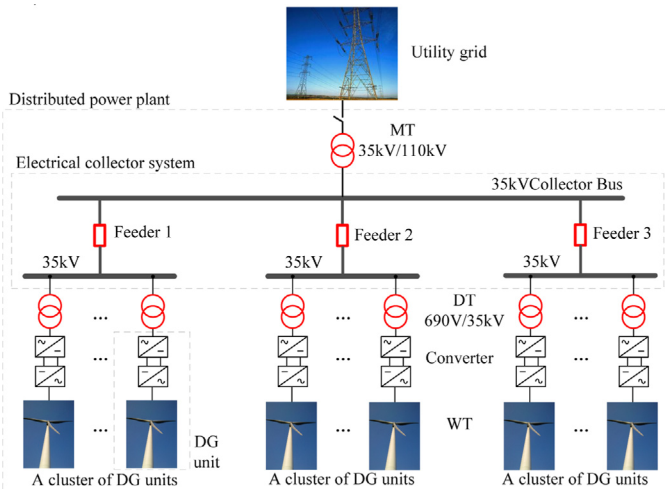

Fig. 1. Typical topology of large-scale distributed power plant.

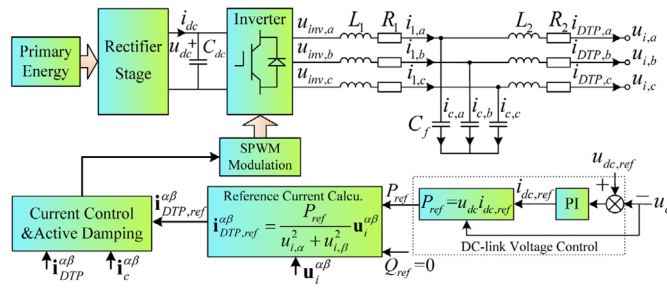

Fig. 2. Overall control diagram of typical distributed inverter.

figured out in [7,16] has been utilized to explore the harmonic characteristics of the output current of the plant. However, neither the detailed models of feeders, DTs, and DG units nor the topology of multiple feeders inside the plant are involved in the process of modeling. The series and parallel resonance problems of harmonic propagation through a long-distance transmission line have been discussed in [17]. However, the harmonic generation side simplified as an ideal harmonic current/voltage source might not exactly describe the wideband-frequency behaviors of the LDPP. The resonances caused by the capacitances and inductances of long transmission cable in offshore wind farms have been investigated in [8,18]. A model of wind farm presented in [19] can be used to determine parallel resonance frequencies. Besides, the models of low-voltage overhead lines and transformers for the discussions of surge protections have been presented in [20,21].

According to aforementioned analysis, the motivation of this study is to build the detailed model of LDPP which can be utilized to fully reveal a variety of resonance phenomena inside the LDPP. The main contributions of this study can be summarized as follows: (1) The model of LDPP, for the first time, has taken the topology of multiple overhead feeders, the distributed capacitances of feeders, the stray capacitances of transformers, and the control strategy of DG units into account at the same time. (2) The model has revealed several resonance bands potentially exist in the wideband-frequency domain inside the LDPP, such as filter resonance band, ring resonance band, and superimposition resonance band. (3) The mechanisms of propagation and magnification of harmonic currents inside the LDPP have been systematically explained. (4) The distributions and movements of several resonance bands along with the length variations of feeders have been vividly illustrated through both theoretical analysis and simulation cases. (5) The methodology of the modeling could provide some suggestions for designers of distributed power plants to avoid specific length of feeders which will drastically magnify characteristic harmonic currents. (6) A hybrid active power filter (HAPF) in order to attenuate wideband-frequency harmonic currents in a typical wind farm has been proposed; also the feasibility of the proposed HAPF has been testified.

2. Large-scale distributed power plant modeling

2.1. Typical topology of large-scale distributed power plant

Fig. 1 shows a typical topology of a LDPP which mainly consists of a main transformer (MT), an electrical collector system, DTs and DG units. The MT acts as a bridge connecting the 35 kV electrical collector system to the 110 kV utility grid. The electrical collector system is composed of three 35 kV overhead feeders which are arranged radially around the 35 kV collector bus. These feeders, especially in mountainous or offshore wind farm, usually extend tens or even hundreds kilometers long. The terminal of each feeder connects with a cluster of DG units through their DTs. In terms of megawatt-level wind turbine, each permanent magnet synchronous generator (PMSG) directly connects with an AC-DC-AC converter, which constitutes a DG unit.

2.2. Modeling of distributed inverter

Fig. 2 shows the overall control diagram of typical distributed inverter. The LCL-type filter is adopted as the output filter of the distributed inverter. Subscripts a, b, c denote the signals expressed in a-b-c coordinate system; Subscripts α, β denote the signals expressed in α-β coordinate system; Subscript ref refers to the signal references. u_{dc}, i_{dc} are the dc-link voltage and current, respectively; C_{dc} is the dc-link capacitor; u_{inv}, u_i are the inverter-output and filter-output voltages, respectively; L_1, L_2 are the inverter-side and grid-side inductors of the LCL-type filter, respectively, and R_1, R_2 are their parasitic resistance, respectively; C_f is the filter capacitor; i_1 is the inverter-side inductor current of the filter; i_{DTP} is the grid-side inductor current of the filter, also refers to the primary windings current of the DT; i_c is the capacitor current of the filter; P, Q are the active and reactive powers, respectively. The bold characters with superscript αβ denote the vectors expressed in α-β coordinate system and arranged as columns, such as

$$\mathbf{i}_{DTP,ref}^{\alpha\beta} = [i_{DTP,ref,\alpha}, i_{DTP,ref,\beta}]^{\mathrm{T}}; \mathbf{i}_{DTP}^{\alpha\beta} = [i_{DTP,\alpha}, i_{DTP,\beta}]^{\mathrm{T}};$$

$$\mathbf{i}_{c}^{\alpha\beta} = [i_{c,\alpha}, i_{c,\beta}]^{\mathrm{T}}; \mathbf{u}_{i}^{\alpha\beta} = [u_{i,\alpha}, u_{i,\beta}]^{\mathrm{T}}.$$

The control diagram of the distributed inverter mainly contains three parts: the dc-link voltage control, the reference current calculating block, and the current control & active damping block. The PI controller and the P_{ref} calculating block are utilized to stabilize the dc-link voltage [13]. Q_{ref} is set to zero for achieving unit power factor.

To simplify the analysis, the current control & active damping block can be given as a single-phase circuit form, such as in [22]. Further, the cascade control loops presented in [3] can be utilized as the detailed control structure for this block, which is composed of a i_{DTP} outer control loop with a proportional resonance (PR) controller and a i_c inner feedback with a proportional feedback coefficient K_C. Thus, the model of the distributed inverter can be deduced as a form of Norton's equivalent circuit, and expressed as

$$I_{DTP}(s) = G_s(s) I_{DTP,ref}(s) - Y_s(s) U_i(s) \quad (1)$$

where $G_s(s)$, $Y_s(s)$ are the equivalent current source coefficient and equivalent admittance of the distributed inverter, respectively, and